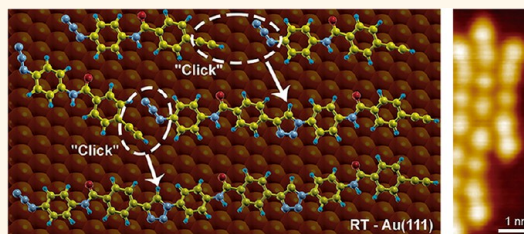


On-Surface Azide–Alkyne Cycloaddition on Au(111)

Oscar Díaz Arado,^{†,*,§} Harry Mönig,^{†,*,*} Hendrik Wagner,[‡] Jörn-Holger Franke,[†] Gernot Langewisch,^{†,‡} Philipp Alexander Held,[‡] Armido Studer,^{‡,*,*} and Harald Fuchs^{†,*,§,||,*}

[†]Physikalisches Institut, Westfälische Wilhelms-Universität Münster, Wilhelm-Klemm-Strasse 10, 48149 Münster, Germany, [‡]Center for Nanotechnology (CeNTech), Heisenbergstrasse 11, 48149 Münster, Germany, [§]Centro de Estudios Avanzados de Cuba (CEAC), Carretera San Antonio de los Baños Km 3 1/2, 17100 La Habana, Cuba, [‡]Organisch-Chemisches Institut, Westfälische Wilhelms-Universität Münster, Corrensstrasse 40, 48149 Münster, Germany, ^{||}Institut für Nanotechnology, Karlsruhe Institute of Technology, 76344 Karlsruhe, Germany, and ^{*}Department of Physics, Université Libre de Bruxelles, Campus Plaine-CP 231, 1050 Brussels, Belgium

ABSTRACT We present [3 + 2] cycloaddition reactions between azides and alkynes on a Au(111) surface at room temperature and under ultrahigh vacuum conditions. High-resolution scanning tunneling microscopy images reveal that these on-surface cycloadditions occur highly regioselectively to form the corresponding 1,4-triazoles. Density functional theory simulations confirm that the reactions can occur at room temperature, where the Au(111) surface does not participate as a catalytic agent in alkyne C–H activation but acts solely as a two-dimensional constraint for the positioning of the two reaction partners. The on-surface azide–alkyne cycloaddition offers great potential toward the development and fabrication of functional organic nanomaterials on surfaces.



KEYWORDS: scanning tunneling microscopy · density functional theory · surface chemistry · on-surface cycloaddition · “click” chemistry · azide–alkyne · on-surface regioselectivity

On-surface chemistry has recently emerged as a powerful tool for the preparation of covalently linked nanostructures at surfaces under ultrahigh vacuum (UHV) conditions.^{1,2} Many of the nanostructures obtained following this route cannot be synthesized *via* classical solution phase synthesis, and therefore, this approach offers a reliable alternative for the preparation of defined supramolecular systems at surfaces. This “bottom-up” approach is very promising for the design of novel materials which show great potential in particular in the field of molecular electronics.^{3–5} The Ullman coupling,^{6,7} condensation of boronic acids,^{8,9} formation of Schiff bases,^{10,11} acylation reactions,^{12,13} and the homocoupling of alkynes^{14,15} are examples of organic reactions which have successfully been conducted under UHV conditions as two-dimensional (2D) processes on single-crystal surfaces. Furthermore, Zhong *et al.* used the geometric constraint of a Au(110) surface to accomplish a dehydrogenative homocoupling reaction between inert alkanes, demonstrating the great potential of on-surface synthesis.¹⁶

Among the many conceivable reactions which have potential to be performed as on-surface processes, cycloadditions (often referred as “click” reactions) are prime candidates along these lines.¹⁷ Such reactions performed as solution phase processes have been used for the modification of surfaces and materials^{18–21} and also for the preparation of biologically active compounds in pharmaceutical research.^{22,23} The most commonly used “click” reaction is the azide–alkyne 1,3-dipolar cycloaddition^{24,25} leading to 1,4- and 1,5-triazoles. Whereas the classical thermal process (Huisgen azide–alkyne [3 + 2] cycloaddition), which proceeds under harsh conditions (*i.e.*, high temperatures), generally delivers a mixture of the two regioisomers, the use of a copper catalyst provides 1,4-triazoles with high efficiency and regioselectivity under ambient conditions (CuAAC).²⁴

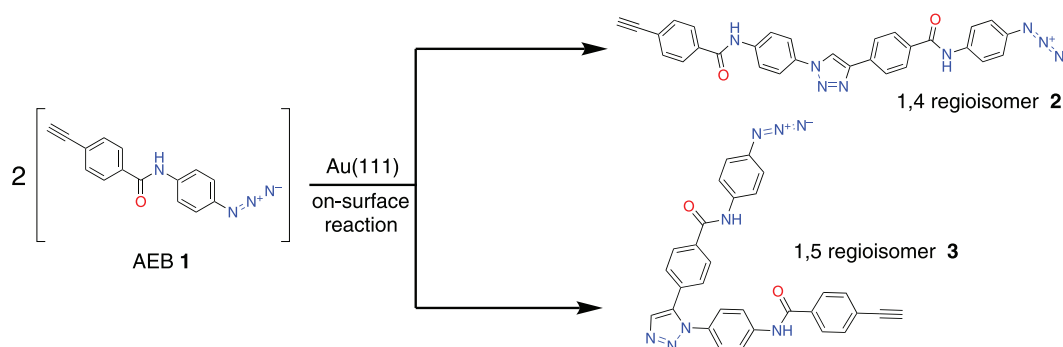
Resembling the CuAAC mechanism in solution, a successful cycloaddition of alkynes and azides was recently accomplished on a Cu(111) surface with complete regioselectivity toward the formation of the corresponding 1,4-triazoles. As for the solution phase process, the high regioselectivity was

* Address correspondence to harry.moenig@uni-muenster.de, studer@uni-muenster.de, fuchsh@uni-muenster.de.

Received for review May 6, 2013 and accepted September 18, 2013.

Published online September 18, 2013
10.1021/nn4022789

© 2013 American Chemical Society



Scheme 1. Proposed on-surface “click” reaction of AEB **1** and possible regioisomeric dimers **2** and **3**.

discussed considering the involvement of a copper acetylide (C–H activation) and bonding of the alkyne group to the Cu(111) surface.²⁶

In the present study, we use a combination of cryogenic scanning tunneling microscopy (STM) and density functional theory (DFT) to investigate on-surface cycloaddition reactions of *N*-(4-azidophenyl)-4-ethynylbenzamide (AEB, **1**) monomers on a Au(111) surface under UHV conditions (see Scheme 1). Our design of the AEB monomers is based on the combination of two phenyl rings connected through an amide linker as the backbone. Such features allow the monomers to be thermally deposited on the surface, where they can lay flat and diffuse, thus increasing the probability of the alkyne and azide groups to meet with each other and react. In addition, the amide linker could form intermolecular hydrogen bonds perpendicular to the targeted reaction direction, making it possible to aim for supramolecular ordering after the deposition and therefore enhance the reaction probability accordingly. Moreover, AEB **1** is charged with an azide and an alkyne moiety, which allows this particular compound to undergo oligomerization. We will show that the “click” reaction on the Au(111) surface occurs under mild conditions at room temperature to provide exclusively the 1,4-regioisomer **2**. The reaction products were manipulated with the STM tip, demonstrating the covalent nature of the bonds formed. DFT simulations clarified the role of the Au(111) surface in the reaction mechanism and in the observed regioselectivity.

RESULTS AND DISCUSSION

Deposition and Reaction on Au(111) at Room Temperature.

AEB **1** was readily prepared using solution phase chemistry as described in the Supporting Information. The deposition of **1** on the Au(111) surface was carried out *via* organic molecular beam deposition (OMBD) at a sublimation temperature of 85 °C (crucible temperature), while the surface was kept at room temperature. The covered surface usually showed a first layer mixture of reactants **1** along with already reacted dimers **2** as well as trimers, surrounded by a disordered molecular phase. Such phase could be ascribed to the azide end group degradation on Au(111) reported by Bebensee *et al.*²⁶

To quantitatively assess the yield of the observed cycloaddition, a representative sampling was chosen out of four different depositions of AEB **1** on Au(111). From a total of 1083 intact molecules observed, 689 (63.3%) were AEB monomers. For the AEB dimer **2** and the trimers, a total of 310 (28.6%) and 84 (7.8%) molecules was identified, respectively. It is interesting to note that the dimerization yield for the cycloaddition on Au(111) is considerably larger than the one observed on Cu(111).²⁶ In Figure 1A, a STM image corresponding to a large coverage deposition of AEB monomers on a Au(111) single crystal kept at room temperature is presented (see also Figure S1).

Figure 1B is a high-resolution image showing a mixture of reacted and unreacted species. A number of monomers were oriented in a way that the alkyne group of one monomer and the azide group of the other were in close proximity and hence properly positioned to undergo the targeted cycloaddition reaction. As it can be seen by the formation of longer linear structures in Figure 1C, along with the buildup of dimers **2** (structure in the middle), the corresponding trimers were also formed. Successful formation of trimers strongly supports the occurrence of the proposed azide–alkyne “click” process since the formation of such trimeric structures should only be feasible if the reaction of the AEB monomer **1** and the dimer **2** occurs between the azide and alkyne end groups of these two reaction partners (see Scheme 1). Moreover, we can rule out the occurrence of Glaser coupling, where the alkyne moieties undergo a dehydrogenative process. Such processes have been recently studied, and it is known to require temperatures considerably larger than 300 K to be triggered.^{14,15}

The inset in Figure 1C represents the molecular structure of a 1,4-triazole dimer **2**. This structure matches very well the STM observations since the alternative 1,5-regioisomer **3** would present a significant tilt (L-shaped structure; see Scheme 1) instead of the observed linear structure. DFT calculations (see below) further confirm the correct assignment of the on-surface dimerization product to structure **2**. It is important to note that for all successful cycloadditions on Au(111), only the formation of the 1,4-regioisomer was

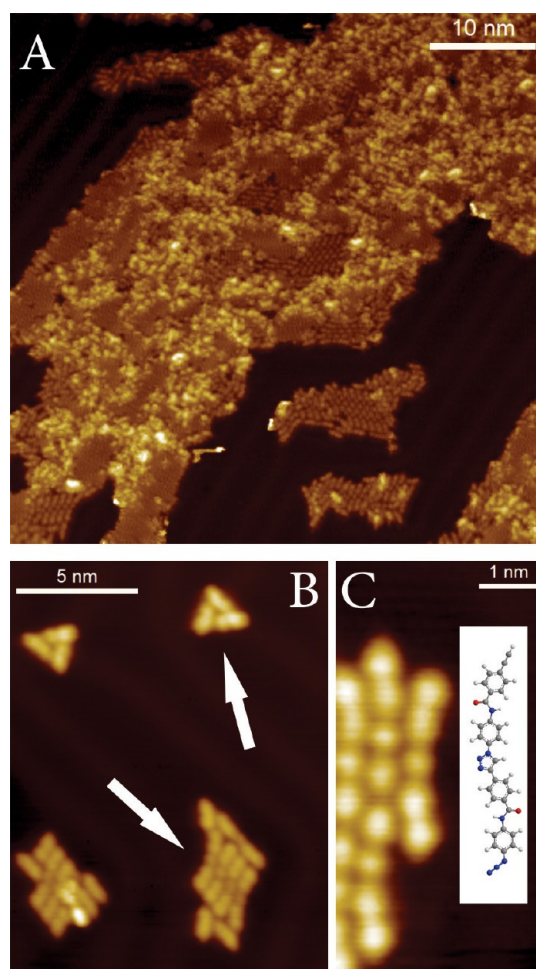


Figure 1. STM images of AEB monomers deposition on Au(111) at room temperature. (A) Large coverage deposition: $50 \times 50 \text{ nm}^2$; $V = 600 \text{ mV}$; $I = 75 \text{ pA}$; $T \leq 78 \text{ K}$. (B) Arrangement of monomers and dimers: $13 \times 17 \text{ nm}^2$; $V = 600 \text{ mV}$; $I = 75 \text{ pA}$; $T \leq 78 \text{ K}$. (C) Dimers and trimers formed as a result of the successful azide-alkyne “click” reaction: $3.5 \times 7 \text{ nm}^2$; $V = 600 \text{ mV}$; $I = 50 \text{ pA}$; $T \leq 5 \text{ K}$. Inset: molecular structure of the 1,4-triazole dimer **2**.

observed and carefully checked by STM. Note that the thermal azide-alkyne cycloaddition in the absence of a Cu catalyst generally requires high temperatures resulting in a mixture of 1,4- and 1,5-triazoles.²⁴ If the cycloaddition products were formed in the crucible during the heating process prior to the deposition and subsequently deposited on the surface, a mixture of both regioisomers is to be expected in the STM observations. Therefore, the observed complete regioselectivity strongly points toward an on-surface reaction. It is likely that the Au substrate used in our experiments somehow lowers the activation energy and also steers the regioselectivity of the [3 + 2] cycloaddition reaction (mechanistic studies will be discussed below).

To exclude the possibility of the reaction occurring during the heating process in the crucible rather than at the Au(111) surface, we conducted two experiments separately. First, mass spectrometry analysis was

performed to investigate the reactivity of monomer **1** toward the thermal cycloaddition (see Figures S2–S4). A stable signal corresponding to the sublimated monomer **1** was detected in a temperature range from 80 to 180 °C, and mass signals corresponding to the dimer **2**, trimers, and/or higher order structures were not detected. Second, dimers **2** were synthesized *ex situ* and sublimated toward the Au(111) surface with the same deposition parameters as with monomer **1**. Mass spectrometry analysis of the heating process and careful inspection of the surface with the STM after the deposition did not show dimers **2** sublimated from the crucible or deposited on the surface (see details in the Supporting Information). Therefore, we exclude the possibility of dimerization during the heating period in the crucible, confirming that the observed dimers **2** and trimers derive from the successful on-surface “click” reactions of **1** on Au(111) under ambient conditions (rt).

Controlled STM Manipulation of the Reacted Oligomers. To confirm the covalent linkage of the reactants, extensive controlled manipulations with the STM tip were carried out on the dimers and the trimers. Figure 2A shows an arrangement of a dimer **2** and two trimers. After a successful manipulation, the dimer was partially detached from the two linear trimers (see Figure 2B). As shown in Figure 2B,C, consecutive manipulations led to a complete separation of the dimer from the two trimers. Importantly, the structure of **2** remained intact after the STM tip manipulations, which proves the covalent nature of the linkage of the two monomers for buildup of the dimeric structure **2**. The amide functionality between the phenyl rings combined with the triazole group in the dimer provides the product large torsional freedom. The trimers could also be successfully manipulated (see Figures S5–S7), although a complete detachment from the adjacent molecules was a challenging task. This can be attributed to the stronger van der Waals forces and probably also to the larger number of hydrogen bonds (between amide bonds) between the linear structures upon switching from the dimer to trimer. These STM manipulations also revealed that AEB dimers **2** and the corresponding trimers display high mechanical stability at the Au(111), which is a typical feature of covalently bonded chemical structures.

Self-Assembly of the Monomers and Reactivity. For the successful on-surface reaction to proceed, two monomers have to diffuse toward each other so that the reactive alkyne and azide functionalities are close enough for successful cycloaddition. Therefore, the self-assembled structure obtained after initial deposition must somehow relate to the reactivity. For example, if the self-assembled structure is in a stable configuration on the surface and as a direct consequence diffusion is too limited, the reaction should be slow or be even suppressed. In our experimental

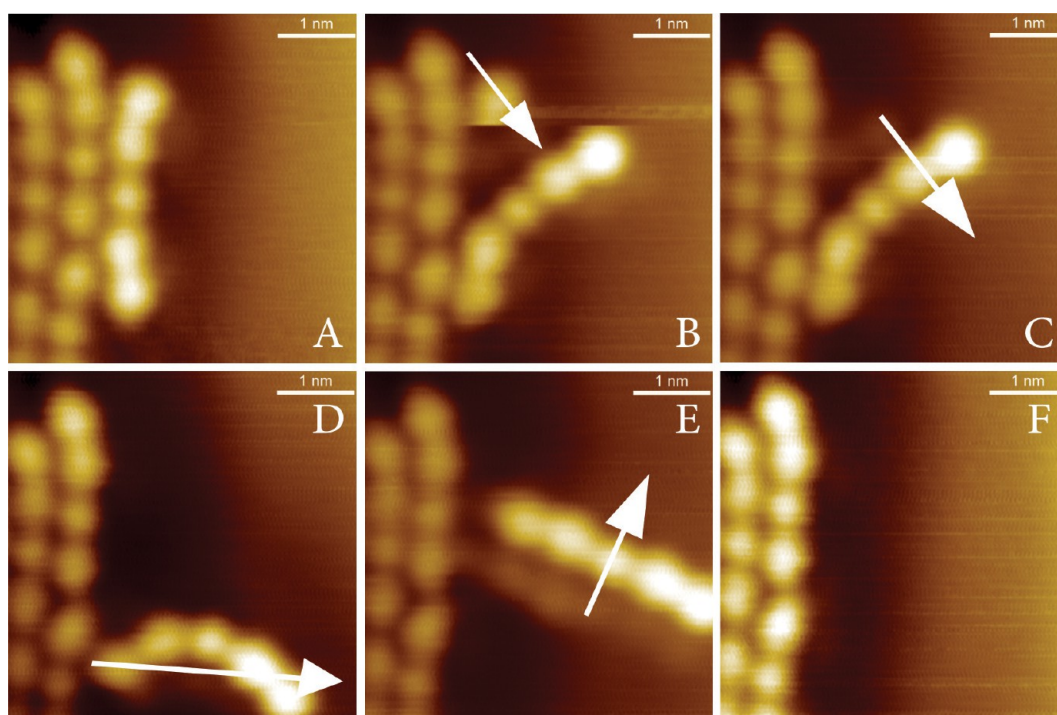


Figure 2. Successful manipulation of a dimer structure **2** with the STM tip. Manipulations were conducted at $T \leq 5$ K with $100 \text{ pA} \leq I \leq 3 \text{ nA}$ and $V = 5 \text{ mV}$. The white arrows represent the manipulation vectors.

studies, in images recorded directly after deposition, we found the unreacted AEB monomers **1** to be present in three different configurations: (i) nucleation along the step edges, which is in agreement with the findings of Bebensee *et al.*,²⁶ who reported that the alkyne group has a high affinity for highly reactive sites, such as step edges; (ii) agglomeration adjacent to molecular islands as a result of diffusion of the molecules on the Au(111) surface and self-assembly steered by van der Waals forces; most likely, those observed monomers are unreacted remnants, which did not find a counterpart to react with (see lower section of Figure 1B); (iii) self-assembled arrangement of three monomers in a stable triangular-shaped island. We found this configuration quite frequently ($\approx 27.4\%$ of the AEB monomers which remain intact after the deposition), being the only configuration where exclusively monomers self-assembled independently (*e.g.*, upper section of Figure 1B).

A high-resolution image of the triangular configuration is shown in Figure 3. It is quite interesting that for molecules which are able to undergo dimerization such stable configuration can be found under similar conditions. However, for most of the on-surface reactions, the pre-arrangement of the reactants is crucial.^{7,15,16} Therefore, one possibility why the reaction does not occur in the triangular configuration is that this particular configuration is too stable and therefore fixed. Moreover, the functional end groups are sterically blocked within this configuration, as

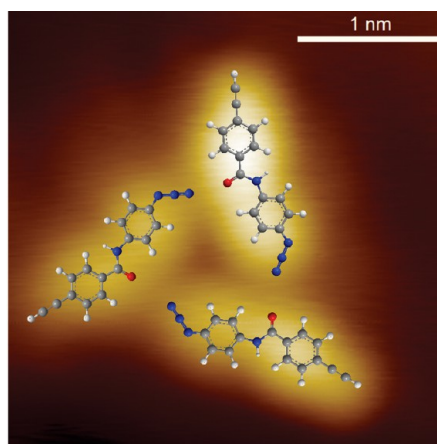


Figure 3. High-resolution image of the self-assembly of three AEB monomers in a triangular arrangement. The inset represents one of the possibilities of how similar end groups that are facing each other would prevent a successful reaction: $3 \times 3 \text{ nm}^2$; $V = 600 \text{ mV}$; $I = 40 \text{ pA}$; $T \leq 5 \text{ K}$.

schematically indicated by the model structure within Figure 3, which leads to reduced reactivity.

Density Functional Theory. In our experiments, we observed successful room temperature on-surface reaction of AEB monomers on Au(111) achieving the corresponding cycloaddition product with complete 1,4-regioselectivity. Since the 1,3-dipolar cycloaddition of azides and alkynes in the absence of a Cu catalyst at elevated temperatures yields a mixture of 1,4- and 1,5-regioisomers, the Au(111) surface seems not only to facilitate the reaction but also to promote a selective formation of one regioisomer. To address this important

question, DFT calculations were carried out to elucidate the on-surface reaction mechanism and to clarify the role of the Au substrate on the regioselectivity.

As a first step, we verified the reactant and the proposed product molecules by comparing the experimental distances with the theoretical values calculated for the gas phase of the monomer **1**, dimer **2**, and trimer (see Figure S8). The center-to-center distance between the two aryl rings of the AEB monomer **1** was found to be 0.65 ± 0.03 nm (calculated, 0.65 nm); for the dimer **2**, the measured distance between the adjacent minima of the 1,4-triazole group is 0.57 ± 0.02 nm (calculated, 0.50 nm); the same distance, measured for the triazoles of the AEB trimer, is 0.55 ± 0.01 and 0.56 ± 0.01 nm (calculated, 0.50 nm), respectively.

Evidently, the triazole groups corresponding to the dimers and trimers have the same size. Therefore, we find not only a good qualitative agreement in the STM images but also a good quantitative agreement between the theoretically and experimentally determined distances. The small differences can be ascribed to the absence of the Au(111) surface in the gas phase calculations, which restrains out-of-plane movements of the molecular components. As a result, bonding angles can differ, which leads to a change of the calculated center-to-center distances.

To understand the reaction mechanism on the Au(111) surface, we performed calculations to estimate the reaction barrier of the on-surface “click” reaction of pre-oriented monomers **1**. To simplify the calculations, we considered *para*-alkynylazidobenzene (*p*-AAB) as a model compound for monomer **1** and first compared the transition state energies of the dimerizations of AEB **1** and the model compound *p*-AAB in vacuum. In a second step, we calculated the transition state energy of the dimerization of *p*-AAB on a flat unreconstructed Au(111) surface (see Figure 4A–C) and compared it with the calculated vacuum barrier. Interestingly, we found that all three calculated barrier heights for the cycloadditions are comparable: the same value (0.72 eV) was calculated for the reaction of the model compound in vacuum and on the Au substrate, and 0.69 eV was obtained for the AEB **1** dimerization in vacuum. This shows that electronic effects exerted by the amide functionality in **1** on the cycloaddition reaction are weak and validates *p*-AAB as an ideal model compound to describe our system. Furthermore, the calculated reaction barriers are low when compared to other on-surface reactions that require temperatures larger than 300 K to be triggered.^{15,16} Our calculated barrier heights thus explain why the reaction can proceed at room temperature in the absence of a catalyst. Moreover, we found that the reaction is strongly exothermic by 2.78 eV for the *p*-AAB in vacuum and on the flat Au(111) substrate and 2.90 eV for the AEB **1** in vacuum.

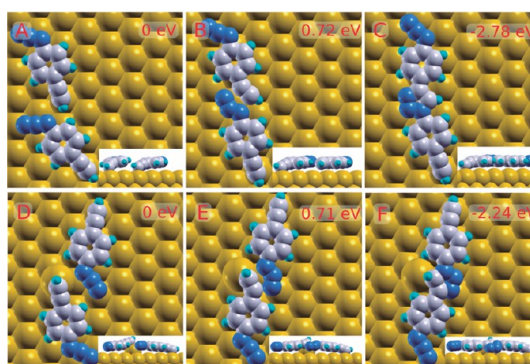


Figure 4. On-surface dimerization of the model compound *p*-AAB on the Au(111) surface. (A–C) Reaction on a flat Au(111) surface. (D–F) Reaction with the reacting terminal carbon atom bound to an additional Au atom on the surface. Initial state energies are defined as 0 eV for both reactions.

The data obtained with the model compound indicate that surprisingly the Au surface seems not to be directly involved in activating the alkyne functionality (for example, by C–H activation, as suggested for the Cu-mediated process). Alkyne groups show a particularly high affinity to bind to surfaces,^{15,26} and it is known from other systems that Au atoms might be pulled out from the surface by organic substrates,²⁷ turning them into activation centers for subsequent on-surface reactions. To assess the potential catalytic role played by the gold atoms of the surface, we simulated the “click” reaction on Au(111) with one uncoordinated additional atom (see Figure 4D–F). To take into account the complete surface reconstruction would require a very large unit cell and therefore resulting in different locations where the molecules could adsorb. The extreme case where a single uncoordinated atom stands out as the most reactive site is more feasible for the calculations and provides valuable information regarding the catalytic role of the surface when compared with the counter extreme case, that is, the flat unreconstructed surface. The strong binding of the alkyne group to the additional gold atom increases the binding energy of the initial state of this configuration by 0.51 eV when compared to the flat surface. However, because of the much weaker interaction with the additional Au atom after the reaction, the exothermicity decreases from 2.78 to 2.24 eV. In this case, the transition state energy is 0.71 eV, barely different from the 0.72 eV calculated for the flat surface. The small difference between these transition state energies indicates only a negligible catalytic effect of uncoordinated Au atoms for the on-surface cycloaddition of *p*-AAB at room temperature. It is reasonable to expect that other surface sites of a herringbone reconstruction will show, at best, a catalytic activity as good as the one observed for the extreme case of an additional uncoordinated Au atom on the surface.

Given the passive role that the Au(111) surface plays in the on-surface reaction of *p*-AAB, which is a good model for AEB **1**, the observed regioselectivity toward the formation of 1,4-regioisomers can be explained in terms of steric hindrance. In solution and in vacuum, the aryl rings next to the 1,5-triazole moiety can rotate in opposite directions, thereby decreasing repulsive steric interactions between the aryl groups.²⁸ On a surface, however, such out-of-plane rotation is in competition with the dispersion forces which favor the conformation where the aryl groups lie flat on the surface coplanar with the triazole ring (see Figure S9). To quantify this effect, we calculated the energy differences between the two possible regioisomers after coupling. We found the 1,5-regioisomer to be less stable than the 1,4 version in vacuum by 0.10 and 0.72 eV on the Au(111) surface. This significant energy difference stemming from steric hindrance between the aryl rings can affect the reaction considerably and increase the transition state energy of the 1,5-regioisomer formation process accordingly. This clearly shows that selectivity of a reaction can be strongly enhanced by moving from a solution phase which proceeds in a three-dimensional space to the analogous on-surface process that occurs as a two-dimensional reaction in confined space. To our knowledge, this is the first report where the beneficial effect of

2D confinement on the selectivity of a reaction is quantitatively explained. We assume this effect to be more general in cases where the surface does not play a catalytic role in the reaction, rendering it as a key factor to control on-surface regioselectivity.

CONCLUSIONS

In conclusion, we showed the successful cycloaddition reaction between terminal alkynes and azides on the Au(111) surface at room temperature and under UHV conditions, with good qualitative and quantitative agreement with the performed DFT calculations. The success of the oligomerization was unambiguously demonstrated through controlled STM tip manipulations without destroying the molecular units. Interestingly, the Au(111) surface does not appear to act as a catalyst for the on-surface reaction to occur at room temperature. However, its role is crucial to orient the molecules before the reaction and to constrain them to a two-dimensional environment. Such constraint explains the observed complete regioselectivity toward the formation of 1,4 regioisomers at a surface. The fact that the regioselectivity of the azide–alkyne cycloaddition can be controlled by the surface constraint and the reactants' design provides an efficient method to develop well-defined nanostructures at surfaces, without the requirement of a catalyst or additional thermal activation.

METHODS

Experiments were performed in a commercial UHV low-temperature STM/AFM (Omicron Nanotechnology) at a base pressure of 1×10^{-10} mbar, which can operate down to liquid helium temperatures. Such setup maintains the sample grounded, while the tip is under a defined potential. The Au(111) single crystal was cleaned by repeated cycles of argon sputtering and subsequent thermal annealing. The AEB compound was evaporated to the substrate under UHV conditions, from a quartz crucible at 85 °C during times from 5 to 35 min, depending on the desired coverage to be obtained.

Mass spectrometry measurements were carried out on a triple quad mass spectrometer, TSQ 7000 (Thermo Finnigan, Bremen, Germany). The compounds were introduced into the EI source via the heatable inlet rod. The electron energy was set at 70 eV, the trap current at 400 μ A, and the source temperature at approximately 185 °C. The compounds were evaporated running a temperature program starting from approximately room temperature up to 400 °C, at a heating rate of 10 °C per minute, while controlling the heating by the total ion count (total TIC controlled evaporation). During the evaporation process, the inlet rod temperature was monitored and recorded together with the acquired mass spectra.

Density functional theory calculations were performed using the plane-wave implementation VASP.^{29–31} The PBE-D functional^{32,33} with the C_6 parameter for Au from Tonigold and Gross³⁴ was used throughout in conjunction with the PAW method. Plane waves up to a cutoff energy of 400 eV were used to represent the wave functions. The Au(111) substrate was represented by a (6 \times 8) supercell three layers thick with the upmost layer free to relax. We modeled the Au substrate as an unreconstructed [1 \times 1] surface. K-point sampling was limited to the Γ point only, and Gaussian broadening of 0.1 eV was used. Molecules are adsorbed on one side of the slab only, and dipole corrections to the energy were carried out accordingly. Ionic relaxation was carried out until all forces were smaller

than 10 meV/Å, with the wave functions converged to energy changes below 10^{-5} eV. Transition states were found with the climbing image nudged elastic band method^{35,36} converged to forces smaller than 20 meV/Å on all images.

Conflict of Interest: The authors declare no competing financial interest.

Acknowledgment. Financial support by the Deutsche Forschungsgemeinschaft (DFG) through the SFB 858 (project B2) and the transregional collaborative research center TRR 061 (projects B3 and B7) is gratefully acknowledged.

Supporting Information Available: Additional details and figures as described in the paper. This material is available free of charge via the Internet at <http://pubs.acs.org>.

REFERENCES AND NOTES

- Gourdon, A. On-Surface Covalent Coupling in Ultrahigh Vacuum. *Angew. Chem., Int. Ed.* **2008**, *47*, 6950–6953.
- Perepichka, D.; Rosei, F. Chemistry: Extending Polymer Conjugation into the Second Dimension. *Science* **2009**, *323*, 216–217.
- Elemans, J.; Lei, S.; De Feyter, S. Molecular and Supramolecular Networks on Surfaces: From Two-Dimensional Crystal Engineering to Reactivity. *Angew. Chem., Int. Ed.* **2009**, *48*, 7298–7333.
- Sakamoto, J.; Van Heijst, J.; Lukin, O.; Schlüter, A. Two-Dimensional Polymers: Just a Dream of Synthetic Chemists? *Angew. Chem., Int. Ed.* **2009**, *48*, 1030–1069.
- Palma, C.-A.; Samori, P. Blueprinting Macromolecular Electronics. *Nat. Chem.* **2011**, *3*, 431–436.
- Lafferentz, L.; Eberhardt, V.; Dri, C.; Africh, C.; Comelli, G.; Esch, F.; Hecht, S.; Grill, L. Controlling On-Surface Polymerization by Hierarchical and Substrate-Directed Growth. *Nat. Chem.* **2012**, *4*, 215–220.

7. Champness, N. Surface Chemistry: Making the Right Connections. *Nat. Chem.* **2012**, *4*, 149–150.
8. Zwaneveld, N.; Pawlak, R.; Abel, M.; Catalin, D.; Gírgmes, D.; Bertin, D.; Porte, L. Organized Formation of 2D Extended Covalent Organic Frameworks at Surfaces. *J. Am. Chem. Soc.* **2008**, *130*, 6678–6679.
9. Dienstmaier, J.; Medina, D.; Dogru, M.; Knochel, P.; Bein, T.; Heckl, W.; Lackinger, M. Isoreticular Two-Dimensional Covalent Organic Frameworks Synthesized by On-Surface Condensation of Diboronic Acids. *ACS Nano* **2012**, *6*, 7234–7242.
10. Weigelt, S.; Busse, C.; Bombis, C.; Knudsen, M.; Gothelf, K.; Strunskus, T.; Wöll, C.; Dahlbom, M.; Hammer, B.; Lægsgaard, E.; *et al.* Covalent Interlinking of an Aldehyde and an Amine on a Au(111) Surface in Ultrahigh Vacuum. *Angew. Chem., Int. Ed.* **2007**, *46*, 9227–9230.
11. Weigelt, S.; Bombis, C.; Busse, C.; Knudsen, M.; Gothelf, K.; Lægsgaard, E.; Besenbacher, F.; Linderroth, T. Molecular Self Assembly from Building Blocks Synthesized on a Surface in Ultrahigh Vacuum: Kinetic Control and Topo-Chemical Reactions. *ACS Nano* **2008**, *2*, 651–660.
12. Treier, M.; Richardson, N.; Fasel, R. Fabrication of Surface-Supported Low-Dimensional Polyimide Networks. *J. Am. Chem. Soc.* **2008**, *130*, 14054–14055.
13. Marele, A.; Mas-Ballesté, R.; Terracciano, L.; Rodríguez-Fernández, J.; Berlanga, I.; Alexandre, S.; Otero, R.; Gallego, J.; Zamora, F.; Gómez-Rodríguez, J. Formation of a Surface Covalent Organic Framework Based on Polyester Condensation. *Chem. Commun.* **2012**, *48*, 6779–6781.
14. Zhang, Y.-Q.; Kepčija, N.; Kleinschrodt, M.; Diller, K.; Fischer, S.; Papageorgiou, A.; Allegretti, F.; Björk, J.; Klyatskaya, S.; Klappenberger, F.; *et al.* Homo-Coupling of Terminal Alkynes on a Noble Metal Surface. *Nat. Commun.* **2012**, *3*, 1286.
15. Gao, H.-Y.; Wagner, H.; Zhong, D.; Franke, J.-H.; Studer, A.; Fuchs, H. Glaser Coupling at Metal Surfaces. *Angew. Chem., Int. Ed.* **2013**, *52*, 4024–4028.
16. Zhong, D.; Franke, J.-H.; Podiyanchari, S.; Blömker, T.; Zhang, H.; Kehr, G.; Erker, G.; Fuchs, H.; Chi, L. Linear Alkane Polymerization on a Gold Surface. *Science* **2011**, *334*, 213–216.
17. Kolb, H.; Finn, M.; Sharpless, K. Click Chemistry: Diverse Chemical Function from a Few Good Reactions. *Angew. Chem., Int. Ed.* **2001**, *40*, 2004–2021.
18. Binder, W.; Sachsenhofer, R. *Macromol. Rapid Commun.* **2007**, *28*, 15–54.
19. Li, Y.; Cai, C. Click Chemistry-Based Functionalization on Non-oxidized Silicon Substrates. *Chem.—Asian J.* **2011**, *6*, 2592–2605.
20. Yao, K.; Tang, C. Controlled Polymerization of Next-Generation Renewable Monomers and Beyond. *Macromolecules* **2013**, *46*, 1689–1712.
21. Casarrubios, L.; De La Torre, M.; Sierra, M. The “Click” Reaction Involving Metal Azides, Metal Alkynes, or Both: An Exploration into Multimetal Structures. *Chem.—Eur. J.* **2013**, *19*, 3534–3541.
22. Kolb, H.; Sharpless, K. The Growing Impact of Click Chemistry on Drug Discovery. *Drug Discovery Today* **2003**, *8*, 1128–1137.
23. Jia, L.; Cheng, Z.; Shi, L.; Li, J.; Wang, C.; Jiang, D.; Zhou, W.; Meng, H.; Qi, Y.; Cheng, D.; *et al.* Fluorine-18 Labeling by Click Chemistry: Multiple Probes in One Pot. *Appl. Radiat. Isot.* **2013**, *75*, 64–70.
24. Rostovtsev, V.; Green, L.; Fokin, V.; Sharpless, K. A Stepwise Huisgen Cycloaddition Process: Copper(I)-Catalyzed Regioselective “Ligation” of Azides and Terminal Alkynes. *Angew. Chem., Int. Ed.* **2002**, *41*, 2596–2599.
25. Tornøe, C.; Christensen, C.; Meldal, M. Peptidotriazoles on Solid Phase: [1,2,3]-Triazoles by Regiospecific Copper(I)-Catalyzed 1,3-Dipolar Cycloadditions of Terminal Alkynes to Azides. *J. Org. Chem.* **2002**, *67*, 3057–3064.
26. Bebensee, F.; Bombis, C.; Vadapoo, S.-R.; Cramer, J.; Besenbacher, F.; Gothelf, K.; Linderroth, T. On-Surface Azide–Alkyne Cycloaddition on Cu(111): Does It “Click” in Ultrahigh Vacuum? *J. Am. Chem. Soc.* **2013**, *135*, 2136–2139.
27. Gao, L.; Liu, Q.; Zhang, Y.; Jiang, N.; Zhang, H.; Cheng, Z.; Qiu, W.; Du, S.; Liu, Y.; Hofer, W.; *et al.* Constructing an Array of Anchored Single-Molecule Rotors on Gold Surfaces. *Phys. Rev. Lett.* **2008**, *101*, 197209.
28. Himo, F.; Lovell, T.; Hilgraf, R.; Rostovtsev, V.; Noodleman, L.; Sharpless, K.; Fokin, V. Copper(I)-Catalyzed Synthesis of Azoles. DFT Study Predicts Unprecedented Reactivity and Intermediates. *J. Am. Chem. Soc.* **2005**, *127*, 210–216.
29. Hafner, J. *Ab-Initio* Simulations of Materials Using VASP: Density-Functional Theory and Beyond. *J. Comput. Chem.* **2008**, *29*, 2044–2078.
30. Kresse, G.; Furthmüller, J. Efficient Iterative Schemes for *Ab Initio* Total-Energy Calculations Using a Plane-Wave Basis Set. *Phys. Rev. B: Condens. Matter Mater. Phys.* **1996**, *54*, 11169–11186.
31. Kresse, G.; Furthmüller, J. Efficiency of *Ab-Initio* Total Energy Calculations for Metals and Semiconductors Using a Plane-Wave Basis Set. *Comput. Mater. Sci.* **1996**, *6*, 15–50.
32. Perdew, J.; Burke, K.; Ernzerhof, M. Generalized Gradient Approximation Made Simple. *Phys. Rev. Lett.* **1996**, *77*, 3865–3868.
33. Grimme, S. Semiempirical GGA-Type Density Functional Constructed with a Long-Range Dispersion Correction. *J. Comput. Chem.* **2006**, *27*, 1787–1799.
34. Tonigold, K.; Gross, A. Adsorption of Small Aromatic Molecules on the (111) Surfaces of Noble Metals: A Density Functional Theory Study with Semiempirical Corrections for Dispersion Effects. *J. Chem. Phys.* **2010**, *132*, 224701.
35. Henkelman, G.; Uberuaga, B.; Jonsson, H. Climbing Image Nudged Elastic Band Method for Finding Saddle Points and Minimum Energy Paths. *J. Chem. Phys.* **2000**, *113*, 9901–9904.
36. Henkelman, G.; Jonsson, H. Improved Tangent Estimate in the Nudged Elastic Band Method for Finding Minimum Energy Paths and Saddle Points. *J. Chem. Phys.* **2000**, *113*, 9978–9985.